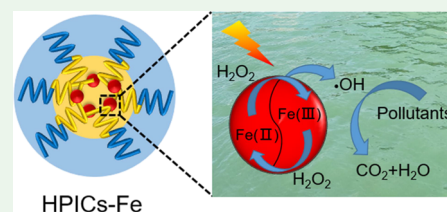


# Hybrid Polymeric Nanostructures Stabilized by Ferric Cations with Photo-Fenton Performance: Implications for Recoverable Multicatalyst Design

Liming Peng, Christophe Mingotaud, Florence Benoît-Marquié,\* and Jean-Daniel Marty\*

**ABSTRACT:** Iron ions, as traditional high-efficiency Fenton reaction catalysts, react with hydrogen peroxide to generate hydroxyl radicals, thereby degrading organic pollutants in wastewater. However, in aqueous solutions, iron ions have a poor chemical stability and are therefore difficult to recover from the reaction medium. We propose that their complexation with double-hydrophilic block copolymers can lead to the formation of nanocatalysts with improved chemical and colloidal stability. Iron ions were added at different molar ratios to a solution of a double-hydrophilic block copolymer, that is, poly(ethylene oxide)-*block*-poly(acrylic acid) to lead to the formation of colloidal structures. Spontaneous formation of highly monodisperse micelles with a hydrodynamic diameter around 25 nm occurs when the charge ratio between the positive iron ions and the negative PAA polyanions is close to one. By combining several techniques, a precise description of the core-shell architecture was achieved. These structures are chemically stable in the pH range of 3–7 and have been successfully used as photo-Fenton catalysts through the degradation of naphthol blue black. Compared to the traditional homogeneous Fenton reaction, these colloidal structures have improved chemical and colloidal stabilities as well as a higher recyclability.

**KEYWORDS:** hybrid polyion complexes, micelle, block copolymer, photo-Fenton, nanocatalyst, colloids



## 1. INTRODUCTION

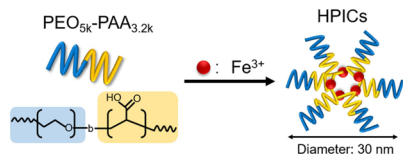
Colloidal nanostructures could be promising catalysts because of their high surface-to-volume ratio merging the benefits of homogeneous (high activity) and heterogeneous catalysis (easy separation). The recovery of such a catalyst is indeed possible by simple ultrafiltration or dialysis, thus meeting one of the most relevant criteria of green catalysis. Hence, catalyst systems based on inorganic nanoparticles<sup>1,2</sup> or metal catalysts complexed with either surfactants or polymers were extensively described in the literature.<sup>3,4</sup> Nevertheless, high-performance nanocatalysts often require complex synthesis processes and specific surfactants or stabilizers.<sup>5–7</sup>

In that context, the use of hybrid polyion complexes (HPICs) (also named hybrid micelles) can be of special interest. These size-controlled nano-objects are obtained from the complexation in aqueous solution of double-hydrophilic block copolymers with charged polyvalent metal ions (e.g., Cu<sup>II</sup>, Gd<sup>III</sup>...). Their hydrodynamic diameter is often well-defined, and they present a high colloidal stability in aqueous solution.<sup>8–10</sup> HPICs have been thus used to induce the formation of well-controlled nanocatalysts. Using HPICs obtained from the complexation of poly(ethylene oxide)-*block*-poly(acrylic acid), PEO-*b*-PAA, block copolymer, and Au<sup>III</sup> as a template, Seo et al.<sup>11</sup> reported the formation of gold nanoparticles, which can efficiently catalyze the reduction of a series of nitroarenes. Additionally, HPICs formed by the complexation of PEO-*b*-PAA and Cu<sup>2+</sup> ions exhibited good

catalytic activity in the degradation of organic compounds based on a Fenton-like mechanism.<sup>12</sup> Such pioneering studies have paved the way to nanostructures that are easy to synthesize and stable and have high potential as catalysts. We aimed here at demonstrating that such objects can lead to the formation of a size-controlled iron-based efficient catalyst. Indeed, the transition metal iron, as a traditional high-efficiency Fenton reaction catalyst, can react with hydrogen peroxide to generate hydroxyl radicals, thereby degrading organic pollutants in wastewater. However, the disadvantage of the iron catalyst is its poor chemical stability, which slows down the generation rate of hydroxyl radicals and reduces the degradation effect.<sup>13,14</sup> In addition, as a homogeneous catalyst, it is difficult to recover from the mixed solution, which recontaminates the aqueous solution and severely limits its development in the field of catalysis.<sup>15,16</sup> With the objective to enhance the stability and recoverability of Fe<sup>3+</sup> ions, we studied here iron-based nanocatalysts issued from the complexation of Fe<sup>3+</sup> ions and PEO<sub>5k</sub>-*b*-PAA<sub>3,2k</sub> block copolymers as illustrated

in Scheme 1. The morphology and colloidal stability of these iron-based colloids were characterized. The photo-Fenton

### Scheme 1. Synthesis of HPICs



catalytic activity and the stability and recoverability of these nanostructures were then investigated.

## 2. EXPERIMENTAL SECTION

**2.1. Chemicals.** PEO<sub>5k</sub>-*b*-PAA<sub>3.2k</sub> was purchased from Polymer Source and used as received. FeCl<sub>3</sub>·6H<sub>2</sub>O, FeCl<sub>2</sub>·4H<sub>2</sub>O, CuSO<sub>4</sub>·5H<sub>2</sub>O, *o*-phenanthroline, NH<sub>3</sub>OHCl, H<sub>2</sub>O<sub>2</sub>, NaOH, HCl, methanol (MeOH), NH<sub>4</sub>OH, and naphthol blue black (noted AB1) were purchased from Sigma-Aldrich. Water was purified through a filter and ion exchange resin by using a Purite device (resistivity 18.2 MΩ cm).

**2.2. Preparation of HPICs Solutions.** HPICs formation was studied with a constant concentration of PEO<sub>5k</sub>-*b*-PAA<sub>3.2k</sub> (0.1 wt%) and increasing amount of FeCl<sub>3</sub> to set  $R = 3 \cdot [\text{Fe}^{3+}] / [\text{AA}^-]$  from 0 to 3. The samples were then adjusted to various pH values with HCl solution (0.1 mol·L<sup>-1</sup>) or NaOH solution (0.1 mol·L<sup>-1</sup>). HPICs-Fe samples with different *R* values were subjected to UV-vis spectroscopy and dynamic light scattering (DLS) testing after stirring for 30 min at room temperature. In the absence of the polymer PEO<sub>5k</sub>-*b*-PAA<sub>3.2k</sub>, free Fe<sup>3+</sup> samples with the same concentration as HPICs-Fe with different *R* values were prepared and analyzed by UV-vis spectroscopy. The synthesis method of the HPICs-Cu solution is the same as that of HPICs-Fe. Note that for HPICs-Cu, *R* is defined as  $2 \cdot [\text{Cu}^{2+}] / [\text{AA}^-]$ .

**2.3. Preparation of Fe<sub>3</sub>O<sub>4</sub> Nanoparticles.** FeCl<sub>3</sub> and FeCl<sub>2</sub> were added to the solution containing PEO<sub>5k</sub>-*b*-PAA<sub>3.2k</sub> in a molar amount of 2:1 (0.1:0.05 mmol). Argon was bubbled through the solution, and the temperature was raised to 70 °C. After stirring for 10 min, a certain amount of NH<sub>4</sub>OH was added to adjust the pH close to 10, and the stirring was continued for 0.5 h. The solution was then cooled to room temperature.

**2.4. Characterization.** UV/vis spectra were recorded with a HP 8452A diode array spectrometer. The spectra were recorded at room temperature, with 10 mm path length quartz cuvettes. DLS measurements were carried out on Zetasizer Nano-ZS (Malvern Instruments, Ltd., UK), with a 4 mW He-Ne laser ( $\lambda = 633$  nm, light scattering measured at 173°). The correlation function was analyzed via the cumulant method to obtain the Z-average diameter of the colloids and by the general purpose method (NNLS) to obtain the distribution of diffusion coefficients of the solutes. The apparent equivalent hydrodynamic diameter was then determined using the Stokes-Einstein equation. Mean diameter values (analysis in Z-average) were obtained from three different runs of the number plot. Standard deviations were evaluated from diameter distribution. Zeta potential values of HPICs were obtained by the doppler anemometry technique, and the test process requires an electric field to be applied to the entire sample solution. This process was performed on a Zetasizer Nano-ZS (Malvern Instruments, Ltd., UK) using folded capillary cells (DTS 1070) at 25 °C. The carbon-coated copper TEM grid (Ted Pella Inc.) loaded with HPICs (*R* = 1.0) solution of different pH values was dried first and then analyzed with an MET Hitachi HT7700 transmission electron microscope at an accelerating voltage of 80 kV. The diameter size-distribution histograms were determined by using magnified transmission electron microscopy (TEM) images on Nano Measurer software. Fourier transform infrared (FT-IR) spectra were recorded on an Avatar 6700 (Nicolet) instrument. The HPICs solutions (pH = 4) with different *R* values were first freeze-dried into powders. The absorbance of the powder

samples was then measured on the diamond crystals using a Nicolet 6700 FT-IR spectrometer from Thermo Fischer Scientific in ATR mode.

**2.5. Colorimetric Titration.** The content of free iron ions is measured by a classical colorimetric method.<sup>17,18</sup> First, standard solutions of different molar amounts were prepared using FeCl<sub>3</sub>·6H<sub>2</sub>O. Stock solutions of NH<sub>3</sub>OHCl (80 mmol·L<sup>-1</sup>), *o*-phenanthroline (10 mmol·L<sup>-1</sup>), and sodium acetate (100 mmol·L<sup>-1</sup>) were prepared. Standard Fe<sup>3+</sup> solution (0.1 mL), NH<sub>3</sub>OHCl solution (0.1 mL), and *o*-phenanthroline solution (0.1 mL) in turn were added to the sodium acetate buffer solution (1.5 mL), and the absorbance at 510 nm was measured. The same proportions of Fe<sup>3+</sup>/PEO<sub>5k</sub>-*b*-PAA<sub>3.2k</sub> (0.1 mL), NH<sub>3</sub>OHCl solution (0.1 mL), and *o*-phenanthroline solution (0.1 mL) were added to the sodium acetate buffer solution (1.5 mL), and the absorbance of the mixture was measured by UV-vis spectroscopy. The pH-triggered decomposition of HPICs and the Fe<sup>3+</sup> ion release experiment were completed with the  $R = 3 \cdot [\text{Fe}^{3+}] / [\text{AA}^-] = 1$  sample. The appropriate FeCl<sub>3</sub> solution was added to the PEO<sub>5k</sub>-*b*-PAA<sub>3.2k</sub> (0.1 wt%, pH = 7) solution in water. Then the mixture was divided evenly into nine portions, and the pH was adjusted to 0.5–7 with HCl (0.1 mol·L<sup>-1</sup>) or NaOH (0.1 mol·L<sup>-1</sup>). The classical colorimetric method is to be used to detect the content of Fe<sup>3+</sup> ions released.

**2.6. Photo-Fenton Experiments.** For the process of photo-Fenton degradation of AB1, four stock aqueous solutions were prepared: a block PEO<sub>5k</sub>-*b*-PAA<sub>3.2k</sub> copolymer solution ( $7.01 \times 10^{-6}$  mol·L<sup>-1</sup> assuming a molar mass of 8200 for the polymer, pH = 7), FeCl<sub>3</sub>·6H<sub>2</sub>O solution ( $1.85 \times 10^{-2}$  mol·L<sup>-1</sup>), AB1 solution ( $4.78 \times 10^{-4}$  mol·L<sup>-1</sup>), and H<sub>2</sub>O<sub>2</sub> solution ( $3.32 \times 10^{-2}$  mol·L<sup>-1</sup>) prepared from a commercial solution at 30 wt%. The HPICs solution with the *R* value equal to 1 was prepared using FeCl<sub>3</sub>·6H<sub>2</sub>O solution and PEO<sub>5k</sub>-*b*-PAA<sub>3.2k</sub> solution. Iron III ions, AB1, and H<sub>2</sub>O<sub>2</sub> were added to 2 mL of water at a molar ratio of 1:1:40, and their UV-visible spectra were analyzed. The pH value of the solution mixture was adjusted with HCl (0.1 mol·L<sup>-1</sup>) or NaOH (0.1 mol·L<sup>-1</sup>) solutions. Then the degradation reaction was initiated under the irradiation of the SCHOTT KLC 1500 LCD lamp equipped with a halogen reflector lamp type EFR (power 6, aperture E, 600 lumen). The experimental temperature is controlled at 25 °C by the temperature control accessory connected to the UV/Vis spectrometer. The evolution of the UV-vis spectrum of the mixture reflected the photo-Fenton reaction process in real time, and the degradation of AB1 was monitored by the changes of the maximum absorption peak at 618 nm. The degradation level was evaluated using the following formula:

$$\text{AB1 degradation level (\%)} = [1 - (C_t/C_0)] \times 100\%$$

where  $C_0$  is the initial AB1 concentration and  $C_t$  is the AB1 concentration at time *t* in the degradation process. As for the photo-Fenton experiment of free Fe<sup>3+</sup> ions, the method is the same as that for HPICs (*R* = 1.0). The reusability experiments of free iron and HPICs (*R* = 1.0) were carried out at pH = 5. At the end of each reaction, a small amount of high-concentration AB1 solution and H<sub>2</sub>O<sub>2</sub> solution were added to the solution, and then the next cycle experiment was carried out. The recovery experiment of HPICs was started after the photo-Fenton reaction had ended. The mixed solution was stirred at 95 °C for 5 min, and precipitation began to appear gradually. Then the HPICs catalyst was obtained by centrifugation.

## 3. RESULTS AND DISCUSSION

**3.1. Formation of Colloids and Characterization.** In aqueous solution, the Fe<sup>3+</sup> ion has a limited pH stability range: above a pH of 2.5, Fe(OH)<sup>2+</sup>aq, Fe(OH)<sub>2</sub><sup>+</sup>aq, and Fe<sub>2</sub>(OH)<sub>2</sub><sup>4+</sup>aq species are predominant and above a pH of 5, the formation of precipitates of Fe(OH)<sub>3</sub> (s) is evidenced (see Figure S1). Interestingly, mixing Fe<sup>3+</sup> ions with the double-hydrophilic block copolymer, PEO<sub>5k</sub>-*b*-PAA<sub>3.2k</sub>, prevents the formation of such precipitates up to pH 7 as long as the ratio between positive charges of the iron ions and negative ones

due to the ionized or ionizable carboxylic functions of the PAA block, noted  $R$  ( $R = 3.[\text{Fe}^{3+}]/[\text{AA}^-]$ ), remained below 3 (Figure S2).

To understand these observations, the interaction between  $\text{Fe}^{3+}$  ions and AA units was first investigated at different pH values through UV-vis spectroscopy. At pH 2, aqueous solutions of  $\text{Fe}^{3+}$  ions showed absorption bands around 240 and 300 nm relative to  $\text{Fe}(\text{H}_2\text{O})_6^{3+}$ ,  $\text{Fe}(\text{OH})_2^+\text{aq}$ , and  $\text{Fe}(\text{OH})_2^+\text{aq}$  species. These absorption bands are strongly modified with the addition of the polymer (Figure 1a).

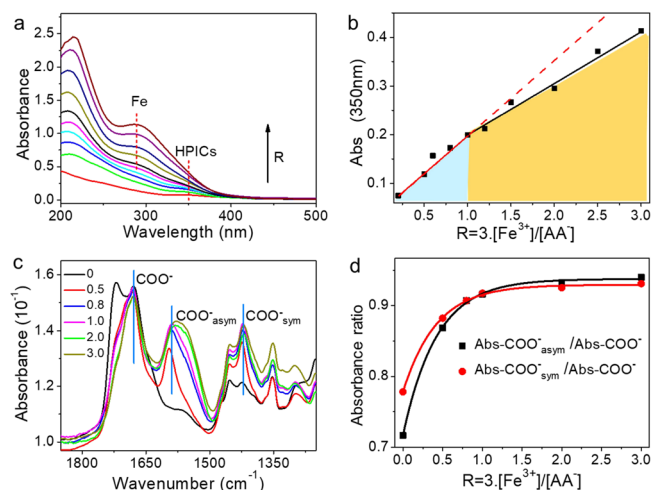


**Figure 1.** (a) UV spectra of polymer/iron solutions (pH = 2) with different  $R$  values corrected from the absorbance of pure  $\text{PEO}_{5k}\text{-}b\text{-PAA}_{3.2k}$  solution; (b) absorbance at 350 nm as a function of the  $R$  value (standard deviation is less than 5% of measured absorbance value). (c) FT-IR spectra of HPICs (pH = 4) with different  $R$  values, and (d) absorbance ratios of symmetric and asymmetric valence vibrational carboxylic groups to the stretched carboxyl groups in HPICs with different  $R$  values.

Following the absorbance at 350 nm, a linear increase of absorbance was measured, and a change of slope was observed at a ratio  $R = 1$  (Figure 1b) after which the measured value of the slope corresponds to the one of free ions (Figure S3). The titration of free  $\text{Fe}^{3+}$  species as a function of  $R$  performed using *o*-phenanthroline comforts this result.<sup>17,18</sup> Hence, while for ratios lower than 1 the addition of iron ions leads to the formation of complexes with the polymer,<sup>19,20</sup> for ratios higher than 1 this addition results in the addition of ions in solution not complexed with the polymer. The same conclusions are obtained at pH 4 starting from a solution comprising different proportion of iron species (and therefore having a different initial absorption spectrum, Figures S4 and S5). Nevertheless, the titration of free  $\text{Fe}^{3+}$  species at pH 4 enables measuring a low amount of such species for  $R > 1$  comparatively to the expected amount. This suggests the presence of highly stable oxo and/or hydroxy species of iron in solution like  $\text{Fe}(\text{OH})_3(\text{s})$  (Figure S6). Interestingly, even if such species were evidenced in solution for  $R > 1$ , the presence of a polymer acting as a stabilizing agent prevents their precipitation. This can explain the absence of precipitates observed at pH 6 (Figure S2).

To further evidence and localize the interactions between iron species and the polymer, FT-IR ATR spectra (Figure 1c) of  $\text{Fe}^{3+}/\text{PEO}_{5k}\text{-}b\text{-PAA}_{3.2k}$  HPICs were measured at different  $R$  values from lyophilized solutions at pH = 4. Prior to analysis, all spectra were normalized to the absorbance of the C=O

stretching band ( $1681\text{ cm}^{-1}$ ) of carboxylic acid groups in  $\text{PEO}_{5k}\text{-}b\text{-PAA}_{3.2k}$  polymers. The peak of the C=O stretching in the COOH groups at  $1720\text{ cm}^{-1}$  of pure  $\text{PEO}_{5k}\text{-}b\text{-PAA}_{3.2k}$  disappeared after interactions with  $\text{Fe}^{3+}$  species, and the asymmetric and symmetrical vibrations of C–O stretching around 1590 and  $1422\text{ cm}^{-1}$  were significantly enlarged, which were all attributed to the strong coordination between  $\text{Fe}^{3+}$  species and carboxylic acid groups.<sup>21,22</sup> The asymmetric vibrational mode of carboxylate near  $1590\text{ cm}^{-1}$  of the sample with  $R = 0.5$  is different from that of other  $R$  value samples (the absorption peak basically does not change after the  $R$  value is greater than 0.8).

Figure 1d showed the ratio of the absorbance of the asymmetric and symmetric valence vibrational carboxylic groups to the stretched carboxyl groups in HPICs with different  $R$  values: when  $0 \leq R \leq 0.5$ , it rises sharply, and then after  $R \geq 0.8$ , it reaches a plateau. This is consistent with previous data on HPICs.<sup>23,24</sup> The evolution of absorbance relative to carboxylate bands measured from FT-IR spectra confirmed the complexation of carboxylic acid function with iron species for the  $R$  ratio up to 1 (or 0.8). With the  $R$  value higher than 1, additional  $\text{Fe}^{3+}$  is present, at least partially, in one of its oxidized form as evidenced from the observed additional peak around  $500\text{ cm}^{-1}$  (Figure S7).

Hence, both UV and FT-IR measurements evidenced an interaction, optimal at a ratio  $R = 1$ , between iron ions and carboxylate functions. To assess the effect of such an interaction on the colloidal properties of the studied system, solutions obtained at different  $R$  ratios were further studied by DLS. Figure S8a shows the evolution of the DLS correlograms of the solutions with the  $R$  ratio at pH 4. A solution of a pure block copolymer is characterized by a very weak scattered intensity, and the corresponding correlogram is associated with a Z-average size above 180 nm (Figure 2a). This was supposedly due to traces of poorly defined self-associations of the copolymers.<sup>23,24</sup>

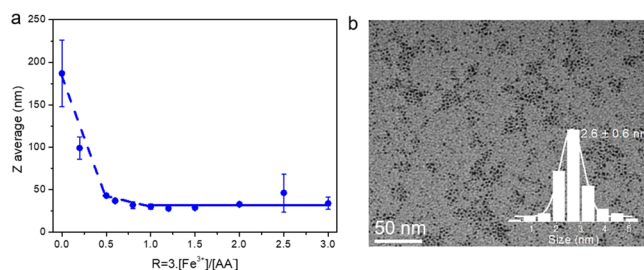


**Figure 2.** (a) Z-average diameter of  $\text{PEO}_{5k}\text{-}b\text{-PAA}_{3.2k}$  solution (0.1 wt %, pH = 4) mixed with different amounts of  $\text{Fe}^{3+}$  at room temperature. (b) TEM image and the corresponding diameter distribution (analyzed by a Gaussian distribution, white line) of a dried solution of HPICs ( $R = 1$  and pH = 4).

The further addition of iron ions induced an increase of the scattered light. This increase is more or less linear with  $R$  up to 1 and is then approximately constant. Such evolution suggests that objects containing several macromolecules were formed by addition of the iron ions until electroneutrality was reached. Analysis of the DLS correlograms reveals a polydisperse population of objects in the solution for  $R$  lower than ca. 0.9. Initially poorly defined polymer self-associations of the copolymers are disaggregated by complexation with iron ions and a clean mono-modal population was measured for  $R$  close

to or higher than 1. Such evolution can be followed as a function of the Z-average diameter of the particles (Figure 2a), for which a clear breaking in the slope versus the ratio  $R$  is recorded around unity with a Z-average diameter measured around  $30 \pm 5$  nm. The formation of colloids is triggered by the addition of iron species and achieved for  $R = 1$ . Such a behavior is similar to the one described with gallium or gadolinium ions and a similar copolymer.<sup>23,24</sup> Hydrodynamic diameters of  $28 \pm 3$  or  $25 \pm 6$  nm (intensity and number average value respectively, Figure S8) were further determined using the NNLS method. These values are comparable to the diameters measured for HPICs formed by  $\text{Gd}^{3+}$ ,  $\text{Cu}^{2+}$ ,  $\text{Ga}^{3+}$ , and  $\text{PAA}_{3k}\text{-}b\text{-PEG}_{6k}$  copolymer.<sup>12,23–25</sup>

The zeta potential measurements versus  $R$  also show (see Figure S9) a change in the slope around  $R = 1$  for which the potential is close to zero. A TEM image of a dried solution of HPICs at pH 4 and  $R = 1$  is shown in Figure 2b. The formation of dense inorganic structures of a small diameter size (below 5 nm) is evidenced with an average diameter measured equal to  $2.6 \pm 0.6$  nm. These results support the formation of nanocolloids induced by the complexation of iron ions and copolymers, with an iron-rich core surrounded by an outer layer of water-soluble polymer chains.<sup>26</sup> For a ratio  $R = 1$ , increasing the pH value of complexation medium from 2 to 7 induces a slight increase of the measured diameter from  $2.1 \pm 0.3$  to  $3.4 \pm 0.6$  nm (see Figure S10).

The chemical stability of these colloids versus the pH was studied in the range of 0.5–7 by measuring the amount of free  $\text{Fe}^{3+}$  ions and Z-average as a function of pH. When the pH is decreased from 7 to 3, almost no released  $\text{Fe}^{3+}$  ion was detected in the solution, and no significant changes in the scattering properties were recorded (Figure 3). Free  $\text{Fe}^{3+}$  in

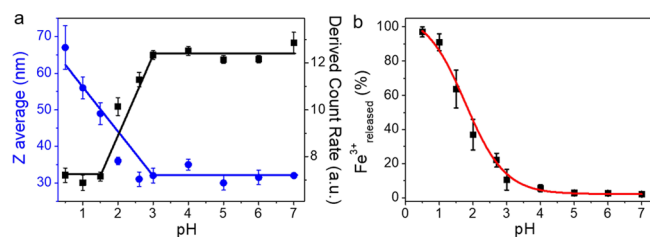


**Figure 3.** (a) Z-average size and scattered intensity of HPICs ( $R = 1.0$ ) at different pH values. (b) Amount of  $\text{Fe}^{3+}$  released from HPICs ( $R = 1.0$ ) as a function of pH.

solution was clearly detected for the pH value lower than 3, and nearly 100% of  $\text{Fe}^{3+}$  was released when pH is around 0.5. Moreover, when the pH was lower than 3, the scattered intensity strongly decreased suggesting the (partial) dissociation of the HPICs colloids. At the same time, the average size is increasing, as already seen for free polymer solutions. These results prove that iron HPICs are highly stable in the pH range of 3–7, lose partially their integrity for a pH range of 1.5–3, and are no longer present for pH lower than 1.5. Moreover, the integrity of colloids was maintained by high-dilution experiments as shown in Figure S11: the size of the colloidal particles did not change significantly after being diluted 10 or even 100 times.

To conclude, the complexation of iron species with polymer  $\text{PEO}_{3k}\text{-}b\text{-PAA}_{3,2k}$  led to the formation of iron-based colloids with a controlled size as illustrated in Scheme 1. The final colloids present a core–shell structure with a core involving

interaction of iron ions with carboxylate and a shell made of the DHBC polymer. The final composition of the core is strongly correlated with the speciation of the iron species present at the considered pH. Finally, these colloids are water-soluble and present an excellent colloidal stability for a pH range between 3 and 7 or upon dilution. These advantages prompted us to study their application in catalysts.

**3.2. Photo-Fenton Reaction.** Naphthol blue black (denoted AB1) is a dye widely used in textiles such as nylon and silk. AB1 contains two azo groups that are not easily decomposed but usually degraded by reactive oxygen species (such as  $\text{HO}_2\cdot$  and  $\text{HO}\cdot$  radicals) generated by the Fenton reaction.<sup>27,28</sup> Its degradation process and mechanism have been previously reported and involved the intermediate formation of aniline, 4-nitroaniline, and naphthylamine.<sup>29,30</sup> In this study, the iron-based polyionic complexes were used as photo-Fenton catalysts and naphthol blue black as a simulated pollutant to test the catalytic performance of HPICs. The above experimental results prove that HPICs are formed when  $R = 1.0$ . To prevent the presence of free  $\text{Fe}^{3+}$  in the solution when  $R$  is greater than 1.0, HPICs samples with  $R = 1$  were selected for the photo-Fenton experiments. The molar ratio of iron III ions:AB1:hydrogen peroxide was set to 1:1:40 as in a previous paper.<sup>31</sup> To analyze the catalytic effect of the iron III HPICs, the degradation of AB1 was followed by UV–visible absorption under light irradiation (see Figure 4a). Figure 4b

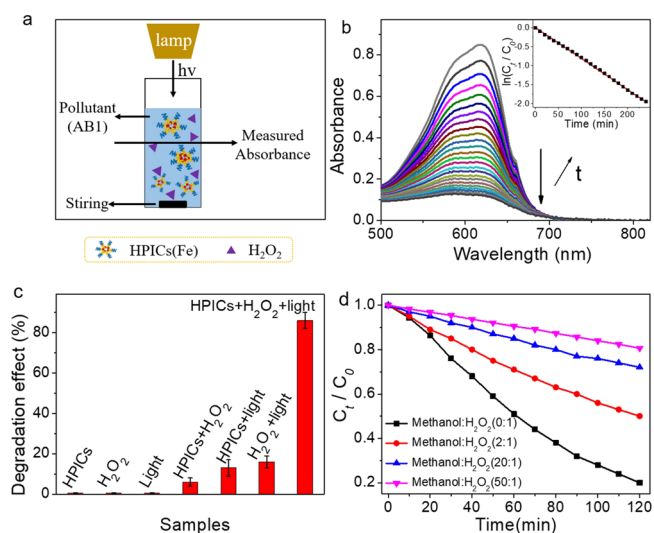


**Figure 4.** (a) Schematic diagram of the photo-Fenton experiment process. (b) Evolution of the absorption spectrum and evolution of the normalized AB1 concentration noted  $C_t/C_0$  (inset) as a function of time in the presence of HPICs ( $R = 1.0$ ), pH = 5. (c) AB1 degradation level under different conditions (pH = 5, 4 h of irradiation). (d) Evolution of relative concentration of AB1  $C_t/C_0$  as a function of time for different molar amounts of methanol (standard deviation associated with the measurement of  $C_t/C_0$  is less than 5%).

shows that the evolution of the UV–Vis spectrum of the solution with time after HPICs ( $R = 1$ ) were added as a photo-Fenton catalyst. This evolution can be analyzed by a pseudo-first-order kinetic mechanism because the logarithm of the AB1 concentration  $C_t$  normalized by its initial concentration  $C_0$  decreased linearly with time (see the inset in Figure 4b). The conversion of the reaction after 4 h was equal to 86%. In the presence of the catalyst alone,  $\text{H}_2\text{O}_2$  alone or light alone, no or very little degradation of AB1 was detected (see Figure 4c).

Combining HPICs with H<sub>2</sub>O<sub>2</sub> or HPICs with light or H<sub>2</sub>O<sub>2</sub> with light enables a slight degradation of the dye. High degradation of AB1 was recorded when combining HPICs with H<sub>2</sub>O<sub>2</sub> and light. This suggests that the HPICs colloids act as a catalyst for the photo-Fenton reaction. Subsequently, the degradation effects of HPICs and free Fe<sup>3+</sup> under different pH values were compared. As shown in Figure S12, when the pH was in the range of 3–7, the degradation effect of AB1 was higher with free Fe<sup>3+</sup> than with HPICs. Complexation of irons within a colloid structure is prejudicial to some extent to the catalytic activity. This is expected, because the species AB1 and oxidative species need to diffuse through the polymeric colloids in order to react together. However, HPICs still showed a good degradation level on AB1, proving that the iron-based polyion complex had good catalytic performance.

In addition, the degradation effect of free Fe<sup>3+</sup> and HPICs on AB1 improved at lower pH, which proved that acidic conditions were more conducive to the photo-Fenton reaction. However, when the pH is too low (0.5–2), the high concentration of protons in solution will decrease the generation rates of ferrous ions and hydroxyl radicals and thus the degradation of AB1 as described in the literature.<sup>32</sup> As expected from the disaggregation of the HPICs for pH in the range of 0.5–2, HPICs and free Fe<sup>3+</sup> ion solutions have the same degradation level in this range of pH.

By free radical scavenging experiments, we demonstrate that the main active species responsible for the degradation of AB1 in this photo-Fenton system was the hydroxyl radical HO·. Its formation was first evidenced from its reaction with terephthalic acid that produces a strong fluorescent product (Figure S13).<sup>33–35</sup> Moreover, methanol was chosen as the scavenger for HO·.<sup>36–38</sup> As shown in Figures 4d and S14, when the molar ratio of methanol and H<sub>2</sub>O<sub>2</sub> in the reaction solution was gradually adjusted from 0:1 to 50:1, the degradation effect of AB1 decreased from 80 to 19% within 2 h, which verified that HO· was the main oxidative species for the degradation of AB1 in the HPICs/H<sub>2</sub>O<sub>2</sub> system.

To estimate the reusability and stability of the HPICs catalyst, after each photo-Fenton experiment, a small amount of high-concentration AB1 and H<sub>2</sub>O<sub>2</sub> was added to the solution to restart the next round of cycling experiment. Figure 5 showed that after three cycles of experiments no significant

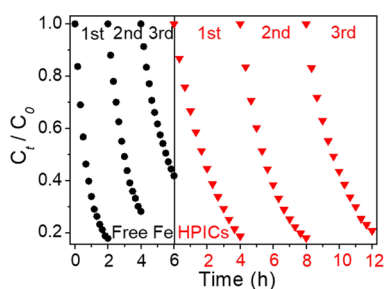


Figure 5. Cycling test of free Fe<sup>3+</sup> and HPICs.

decrease of the degradation level of AB1 can be measured. On the contrary, for free Fe<sup>3+</sup> ions, the degradation effect was significantly reduced after three cycles. Therefore, the block copolymers and the HPICs structure are improving dramatically the reusability of the iron catalysts. Through heating experiments, we found that HPICs precipitated at 95 °C on the contrary to simple iron ions (Figure S15). Consequently,

HPICs can be easily removed from the mixed solution by centrifugation.

Finally, we compared the degradation effect of HPICs-Fe and our previously synthesized copper-based HPICs-Cu on AB1 at different pH values. As shown in Figure S16, under the same conditions, the catalytic activity of HPICs-Fe is much higher than that of HPICs-Cu, again proving the feasibility of iron-based HPICs as water treatment catalysts. Moreover, in order to distinguish the catalytic performance of iron-based hybrid polyionic complexes and iron oxide nanoparticles, Fe<sub>x</sub>O<sub>y</sub> nanoparticles (Figure S17a,b) were also synthesized in the presence of the PEO<sub>5k</sub>-*b*-PAA<sub>3.2k</sub> copolymer under alkaline conditions. The FT-IR spectrum showed bands related to Fe–O bonds (Figure S17c) as well bands associated with N–H groups (the synthesis of Fe<sub>x</sub>O<sub>y</sub> indeed used NH<sub>3</sub>H<sub>2</sub>O to adjust the pH). Then, the photo-Fenton degradation experiment of AB1 at pH = 4 was performed with the same molar amount of HPICs-Fe and Fe<sub>x</sub>O<sub>y</sub> solutions (with respect to iron). The latter show lower catalytic activity therefore demonstrating that, comparatively to the one of Fe<sub>x</sub>O<sub>y</sub>, the HPICs specific structure and composition are prone to favor the catalytic efficiency of iron-based nanocatalysts (Figure S17d). Moreover, even if a strict comparison is difficult because of the numerous parameters involved in this degradation reaction (specific experimental parameters and mechanism), the efficiency of HPICs-Fe competes well with other reported systems involving different mechanisms: Fenton, photo-Fenton, electro-Fenton... (see Table S1).<sup>39,40</sup>

## 4. CONCLUSIONS

The formation of HPICs nanostructures from the complexation of a double-hydrophilic block copolymer PEO<sub>5k</sub>-*b*-PAA<sub>3.2k</sub> with Fe<sup>3+</sup> was successfully demonstrated by means of UV–vis, FT-IR, DLS, and TEM. The hybrid polyionic complex obtained by this simple self-assembly process has a core–shell structure and a hydrodynamic diameter equal to 25 ± 6 nm and is chemically stable in the pH range of 3–7. This iron-based HPICs were successfully used as homogeneous catalysts involving a photo-Fenton degradation reaction of naphthol blue black. For a chosen concentration of catalyst, the measured level of degradation is tenfold higher than that of HPICs-Cu and Fe<sub>x</sub>O<sub>y</sub> nanoparticles. The nanocatalyst has high cycling stability and can be easily recovered by heating/centrifugation or dialysis which provides promising perspectives for the development of Fenton reaction catalysts in the future. Moreover, the ability of HPICs to be formed from different ions or mixture of ions opens promising perspectives to get access to multicatalytic “homogeneous” systems for different reactions (Lewis catalyt...).

## FUNDING

“Agence National pour la Recherche.” ANR Hybrid MRI, n° ANR-19-CE09-0011-01, Centre National de la Recherche Scientifique (CNRS), Université de Toulouse, China Scholarship Council (CSC).

## ASSOCIATED CONTENT

### Supporting Information

The Supporting Information is available free of charge at <https://pubs.acs.org/doi/10.1021/acsnm.2c02501>.

Complementary characterization of HPICs (DLS correlograms, UV spectra, and TEM measurements) and catalytic results (PDF)

## AUTHOR INFORMATION

### Corresponding Authors

Florence Benoit-Marquié – Laboratoire des IMRCP, CNRS UMR 5623, University of Toulouse, 31062 Toulouse, France; [orcid.org/0000-0003-3234-7001](https://orcid.org/0000-0003-3234-7001); Email: [florence.benoit-marquie@univ-tlse3.fr](mailto:florence.benoit-marquie@univ-tlse3.fr)

Jean-Daniel Marty – Laboratoire des IMRCP, CNRS UMR 5623, University of Toulouse, 31062 Toulouse, France; [orcid.org/0000-0001-7631-8865](https://orcid.org/0000-0001-7631-8865); Email: [jean-daniel.marty@univ-tlse3.fr](mailto:jean-daniel.marty@univ-tlse3.fr)

### Authors

Liming Peng – Laboratoire des IMRCP, CNRS UMR 5623, University of Toulouse, 31062 Toulouse, France; [orcid.org/0000-0002-8216-242X](https://orcid.org/0000-0002-8216-242X)

Christophe Mingotaud – Laboratoire des IMRCP, CNRS UMR 5623, University of Toulouse, 31062 Toulouse, France; [orcid.org/0000-0002-9651-6209](https://orcid.org/0000-0002-9651-6209)

Complete contact information is available at: <https://pubs.acs.org/10.1021/acsnm.2c02501>

### Author Contributions

The manuscript was written through contributions of all authors. All authors have given approval to the final version of the manuscript.

### Notes

The authors declare no competing financial interest.

## ACKNOWLEDGMENTS

The author thanks CNRS, University Paul Sabatier and the China Scholarship Council (CSC) for financial support. The authors acknowledge the CMEAB platform for TEM facilities, Corinne Routaboul from the ICT platform for FT-IR experiments, Charles-Louis Serpentine and Diana Ciuculescu-Pradines for scientific discussions.

## REFERENCES

- (1) Crooks, R. M.; Zhao, M. Dendrimer-Encapsulated Pt Nanoparticles: Synthesis, Characterization, and Applications to Catalysis. *Adv. Mater.* **1999**, *11*, 217–220.
- (2) Keilitz, J.; Nowag, S.; Marty, J.-D.; Haag, R. Chirally Modified Platinum Nanoparticles Stabilized by Dendritic Core-Multishell Architectures for the Asymmetric Hydrogenation of Ethyl Pyruvate. *Adv. Synth. Catal.* **2010**, *352*, 1503–1511.
- (3) Wei, Z.; Duan, H.; Weng, G.; He, J. Metals in polymers: hybridization enables new functions. *J. Mater. Chem. C* **2020**, *8*, 15956–15980.
- (4) Bergbreiter, D. E.; Tian, J.; Hongfa, C. Using Soluble Polymer Supports To Facilitate Homogeneous Catalysis. *Chem. Rev.* **2009**, *109*, 530–582.
- (5) Albuquerque, B. L.; Denicourt-Nowicki, A.; Mériade, C.; Domingos, J. B.; Roucoux, A. Water soluble polymer–surfactant complexes-stabilized Pd(0) nanocatalysts: Characterization and structure–activity relationships in biphasic hydrogenation of alkenes and  $\alpha,\beta$ -unsaturated ketones. *J. Catal.* **2016**, *340*, 144–153.
- (6) Mévellec, V.; Roucoux, A.; Ramirez, E.; Philippot, K.; Chaudret, B. Surfactant-Stabilized Aqueous Iridium(0) Colloidal Suspension: An Efficient Reusable Catalyst for Hydrogenation of Arenes in Biphasic Media. *Adv. Synth. Catal.* **2004**, *346*, 72–76.
- (7) Polepalli, S.; Rao, C. P. Drum Stick Seed Powder as Smart Material for Water Purification: Role of Moringa oleifera Coagulant Protein-Coated Copper Phosphate Nanoflowers for the Removal of Heavy Toxic Metal Ions and Oxidative Degradation of Dyes from Water. *ACS Sustainable Chem. Eng.* **2018**, *6*, 15634–15643.
- (8) Gérardin, C.; Sanson, N.; Bouyer, F.; Fajula, F.; Putaux, J.-L.; Joanicot, M.; Chopin, T. Highly Stable Metal Hydrous Oxide Colloids by Inorganic Polycondensation in Suspension. *Am. Ethnol.* **2003**, *115*, 3809–3813.
- (9) Shin, H. W.; Sohn, H.; Jeong, Y. H.; Lee, S. M. Construction of Paramagnetic Manganese-Chelated Polymeric Nanoparticles Using Pyrene-End-Modified Double-Hydrophilic Block Copolymers for Enhanced Magnetic Resonance Relaxivity: A Comparative Study with Cisplatin Pharmacophore. *Langmuir* **2019**, *35*, 6421–6428.
- (10) Nishiyama, N.; Yokoyama, M.; Aoyagi, T.; Okano, T.; Sakurai, Y.; Kataoka, K. Preparation and Characterization of Self-Assembled Polymer–Metal Complex Micelle from cis-Dichlorodiammineplatinum(II) and Poly(ethylene glycol)–Poly( $\alpha,\beta$ -aspartic acid) Block Copolymer in an Aqueous Medium. *Langmuir* **1999**, *15*, 377–383.
- (11) Seo, E.; Kim, J.; Hong, Y.; Kim, Y. S.; Lee, D.; Kim, B.-S. Double Hydrophilic Block Copolymer Templated Au Nanoparticles with Enhanced Catalytic Activity toward Nitroarene Reduction. *J. Phys. Chem. C* **2013**, *117*, 11686–11693.
- (12) Mestivier, M.; Li, J. R.; Camy, A.; Frangville, C.; Mingotaud, C.; Benoit-Marquié, F.; Marty, J. D. Copper-Based Hybrid Polyion Complexes for Fenton-Like Reactions. *Chemistry* **2020**, *26*, 14152–14158.
- (13) Zhang, G.; Gao, Y.; Zhang, Y.; Guo, Y. Fe<sub>2</sub>O<sub>3</sub>-Pillared Rectorite as an Efficient and Stable Fenton-Like Heterogeneous Catalyst for Photodegradation of Organic Contaminants. *Environ. Sci. Technol.* **2010**, *44*, 6384–6389.
- (14) Ye, Z.; Schukraft, G. E. M.; L’Hermitte, A.; Xiong, Y.; Brillas, E.; Petit, C.; Sirés, I. Mechanism and stability of an Fe-based 2D MOF during the photoelectro-Fenton treatment of organic micropollutants under UVA and visible light irradiation. *Water Res.* **2020**, *184*, No. 115986.
- (15) Sabhi, S.; Kiwi, J. Degradation of 2,4-dichlorophenol by immobilized iron catalysts. *Water Res.* **2001**, *35*, 1994–2002.
- (16) Cole-Hamilton David, J. Homogeneous Catalysis—New Approaches to Catalyst Separation, Recovery, and Recycling. *Science* **2003**, *299*, 1702–1706. (accessed 2021/09/12)
- (17) Pyenson, H.; Tracy, P. H. A 1,10—Phenanthroline Method for the Determination of Iron in Powdered Milk. *J. Dairy Sci.* **1945**, *28*, 401–412.
- (18) Haviv, A. H.; Grenèche, J.-M.; Lellouche, J.-P. Aggregation Control of Hydrophilic Maghemite ( $\gamma$ -Fe<sub>2</sub>O<sub>3</sub>) Nanoparticles by Surface Doping Using Cerium Atoms. *J. Am. Chem. Soc.* **2010**, *132*, 12519–12521.
- (19) Adamek, E.; Baran, W.; Sobczak, A. Effect of FeCl<sub>3</sub> on the photocatalytic processes initiated by UVA and vis light in the presence of TiO<sub>2</sub>-P<sub>25</sub>. *Appl. Catal., B* **2015**, *172–173*, 136–144.
- (20) Basavegowda, N.; Somai Magar, K. B.; Mishra, K.; Lee, Y. R. Green fabrication of ferromagnetic Fe<sub>3</sub>O<sub>4</sub> nanoparticles and their novel catalytic applications for the synthesis of biologically interesting benzoxazinone and benzthioxazinone derivatives. *New J. Chem.* **2014**, *38*, 5415–5420.
- (21) Bronstein, L. M.; Huang, X.; Retrum, J.; Schmucker, A.; Pink, M.; Stein, B. D.; Dragnea, B. Influence of Iron Oleate Complex Structure on Iron Oxide Nanoparticle Formation. *Chem. Mater.* **2007**, *19*, 3624–3632.
- (22) Świdorski, G.; Wilczewska, A. Z.; Świsłocka, R.; Kalinowska, M.; Lewandowski, W. Spectroscopic (IR, Raman, UV–Vis) study and thermal analysis of 3d-metal complexes with 4-imidazolecarboxylic acid. *J. Therm. Anal. Calorim.* **2018**, *134*, 513–525.
- (23) Frangville, C.; Li, Y.; Billotey, C.; Talham, D. R.; Taleb, J.; Roux, P.; Marty, J. D.; Mingotaud, C. Assembly of Double-Hydrophilic Block Copolymers Triggered by Gadolinium Ions: New Colloidal MRI Contrast Agents. *Nano Lett.* **2016**, *16*, 4069–4073.

- (24) Gineste, S.; Lonetti, B.; Yon, M.; Giermanska, J.; Di Cola, E.; Sztucki, M.; Coppel, Y.; Mingotaud, A. F.; Chapel, J. P.; Marty, J. D.; Mingotaud, C. Hybrid polymeric micelles stabilized by gallium ions: Structural investigation. *J. Colloid Interface Sci.* **2022**, *609*, 698–706.
- (25) Yon, M.; Gineste, S.; Parigi, G.; Lonetti, B.; Gibot, L.; Talham, D. R.; Marty, J.-D.; Mingotaud, C. Hybrid Polymeric Nanostructures Stabilized by Zirconium and Gadolinium Ions for Use as Magnetic Resonance Imaging Contrast Agents. *ACS Appl. Nano Mater.* **2021**, *4*, 4974–4982.
- (26) Sanson, N.; Bouyer, F.; Destarac, M.; In, M.; Gerardin, C. Hybrid polyion complex micelles formed from double hydrophilic block copolymers and multivalent metal ions: size control and nanostructure. *Langmuir* **2012**, *28*, 3773–3782.
- (27) Ozcan, A. A.; Ozcan, A. Investigation of applicability of Electro-Fenton method for the mineralization of naphthol blue black in water. *Chemosphere* **2018**, *202*, 618–625.
- (28) Ferkous, H.; Merouani, S.; Hamdaoui, O. Sonolytic degradation of naphthol blue black at 1700 kHz: Effects of salts, complex matrices and persulfate. *J. Water Process. Eng.* **2016**, *9*, 67–77.
- (29) Debnath, S.; Ballav, N.; Nyoni, H.; Maity, A.; Pillay, K. Optimization and mechanism elucidation of the catalytic photo-degradation of the dyes Eosin Yellow (EY) and Naphthol blue black (NBB) by a polyaniline-coated titanium dioxide nanocomposite. *Appl. Catal., B* **2015**, *163*, 330–342.
- (30) Ball, M. T.; Hay, J.; Masrouji, H. M.; Sugden, J. K. Photochemical degradation of C.I. acid black 1. *Dyes Pigm.* **1992**, *19*, 51–57.
- (31) Haddou, M.; Benoit-Marquié, F.; Maurette, M.-T.; Oliveros, E. Oxidative Degradation of 2,4-Dihydroxybenzoic Acid by the Fenton and Photo-Fenton Processes: Kinetics, Mechanisms, and Evidence for the Substitution of H<sub>2</sub>O<sub>2</sub> by O<sub>2</sub>. *Helv. Chim. Acta* **2010**, *93*, 1067–1080.
- (32) Neyens, E.; Baeyens, J. A review of classic Fenton's peroxidation as an advanced oxidation technique. *J. Hazard. Mater.* **2003**, *98*, 33–50.
- (33) Guo, T.; Wang, K.; Zhang, G.; Wu, X. A novel  $\alpha$ -Fe<sub>2</sub>O<sub>3</sub>@g-C<sub>3</sub>N<sub>4</sub> catalyst: Synthesis derived from Fe-based MOF and its superior photo-Fenton performance. *Appl. Surf. Sci.* **2019**, *469*, 331–339.
- (34) Hu, J.; Zhang, P.; An, W.; Liu, L.; Liang, Y.; Cui, W. In-situ Fe-doped g-C<sub>3</sub>N<sub>4</sub> heterogeneous catalyst via photocatalysis-Fenton reaction with enriched photocatalytic performance for removal of complex wastewater. *Appl. Catal., B* **2019**, *245*, 130–142.
- (35) Ortega-Liebana, M. C.; Hueso, J. L.; Larrea, A.; Sebastian, V.; Santamaria, J. Ferroxyhyte nanoflakes coupled to up-converting carbon nanodots: a highly active, magnetically recoverable, Fenton-like photocatalyst in the visible-NIR range. *Chem. Commun.* **2015**, *51*, 16625–16628.
- (36) Xiao, S.; Zhou, C.; Ye, X.; Lian, Z.; Zhang, N.; Yang, J.; Chen, W.; Li, H. Solid-Phase Microwave Reduction of WO<sub>3</sub> by GO for Enhanced Synergistic Photo-Fenton Catalytic Degradation of Bisphenol A. *ACS Appl. Mater. Interfaces* **2020**, *12*, 32604–32614.
- (37) Su, L.; Wang, P.; Ma, X.; Wang, J.; Zhan, S. Regulating Local Electron Density of Iron Single Sites by Introducing Nitrogen Vacancies for Efficient Photo-Fenton Process. *Angew. Chem., Int. Ed. Engl.* **2021**, *60*, 21261–21266.
- (38) Wang, N.; Ma, W.; Du, Y.; Ren, Z.; Han, B.; Zhang, L.; Sun, B.; Xu, P.; Han, X. Prussian Blue Microcrystals with Morphology Evolution as a High-Performance Photo-Fenton Catalyst for Degradation of Organic Pollutants. *ACS Appl. Mater. Interfaces* **2019**, *11*, 1174–1184.
- (39) Sun, J.-H.; Sun, S.-P.; Wang, G.-L.; Qiao, L.-P. Degradation of azo dye Amido black 10B in aqueous solution by Fenton oxidation process. *Dyes Pigm.* **2007**, *74*, 647–652.
- (40) Xie, C.; Wen, X.; Xiao, C.; Wei, S.; Wu, X.; Liu, S.; Cao, J. Copper Nanoclusters/Red Globe Flower Carbon as a Fenton-Like Catalyst for the Degradation of Amido Black 10B. *Water, Air, Soil Pollut.* **2020**, *231*, 280.